Geochemical Perspectives Letters

Potential of Earth's core as a reservoir for noble gases: Case for helium and neon

M.A. Bouhifd[1,2*], A.P. Jephcoat[2,3], D. Porcelli[2], S.P. Kelley[4,§], B. Marty[5]

OPEN ACCESS
doi: 10.7185/geochemlet.2028

Abstract

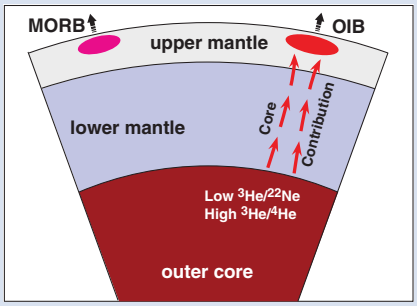

This study investigates metal–silicate partitioning of neon (D_{Ne}) under the likely conditions of early Earth's core formation: up to 16 GPa, ~ 3000 K and an oxygen fugacity near IW-2 (2 log units below the Iron-Wüstite buffer). We find that the D_{Ne} coefficients range between 10^{-2} and 10^{-1}. These partition coefficients are only one of the controlling factors of noble gas distributions within the early Earth: because, even if D_{He} and D_{Ne} are low (~10^{-4}), there may have been sufficient noble gases present in the mantle to supply a significant quantity of He and Ne to the core. Assuming gas-melt equilibrium of the molten proto-Earth with a nebular gas composition and concomitant metal-silicate differentiation, the core would have inherited and maintained throughout Earth's history high $^3He/^4He$ ratios and low $^3He/^{22}Ne$ ratios (<0.6), making the core a potential source of primordial light noble gases in mantle plumes.

Received 13 December 2019 | Accepted 6 August 2020 | Published 9 September 2020

Letter

Earth's mantle contains a mixture of primordial noble gases, in particular solar-type helium and neon, and radiogenic noble gases (*e.g.*, Marty, 2012; Moreira, 2013). The isotopic ratios of He and Ne in ocean island basalts (OIB) indicate the existence of a reservoir with high concentrations of primordial noble gases in the deep Earth. This reservoir appears to have been isolated from the MORB (Mid-Ocean Ridge Basalts) source reservoir 4.4 billion years ago (*e.g.*, Pepin and Porcelli, 2006; Mukhopadhyay, 2012; and references therein).

The origin of high $^3He/^4He$ and low $^3He/^{22}Ne$ ratios in many OIBs is still much debated and there has long been a supposition that OIBs sample a primordial and undegassed reservoir located in the deep mantle. Increasing evidence for mantle convection processes has pushed the debated boundary for a primitive mantle source location ever deeper into the lower mantle, reaching the core-mantle boundary (*e.g.*, Williams *et al.*, 2019). The Earth's core has also been suggested as an alternative source of noble gases (Porcelli and Halliday, 2001; Trieloff and Kunz, 2005; Armytage *et al.*, 2013; Bouhifd *et al.*, 2013; Roth *et al.*, 2019).

Extending our previous work on helium, here we investigate neon partitioning between molten silicates and Fe-rich alloy liquids up to 16 GPa and to a maximum temperature of ~3000 K. We also address the behaviour of He/Ne in an early magma ocean.

A CI-chondrite model composition was chosen for the starting silicate material (*e.g.*, Bouhifd *et al.*, 2013). To simulate Earth's core formation under conditions of segregation from a deep magma ocean, we performed experiments with a starting mix of CI-chondrite glass (66 wt. %) with various Fe-rich alloys (34 wt. %).

We used a set-up described in previous studies (*e.g.*, Jephcoat *et al.*, 2008) with all details reported in the Supplementary Information. Briefly, we used diamond anvils with 500 μm culets, and stainless steel gaskets pre-indented to a thickness of ~50 μm and drilled to a diameter of ~100 μm. Samples were mounted in the pressure chamber and neon was loaded with a high pressure gas-loading technique at 200 MPa. Pressures were measured using the ruby fluorescence method before and after each heating stage. The samples were heated by a 100 W air-cooled fibre laser with emission centred at 1070 nm for an average of about 15 minutes for each zone of the sample. During the heating stage the surrounding neon melted by conductive heating from the heated sample, allowing its dissolution into the sample. Temperatures were determined spectro-radiometrically with a fit to a grey-body Planck function. The temperatures of our runs were higher by at least 200 degrees than the liquidus temperature of peridotite (Zhang and Herzberg, 1994; Fig. S-2). Because our experiments are not routine the success of our LHDAC technique was demonstrated in our previous studies where we found a good agreement between

1. Laboratoire Magmas et Volcans, Université Clermont Auvergne, CNRS UMR 6524, OPGC-IRD, F-63000 Clermont-Ferrand, France
2. University of Oxford, Department of Earth Sciences, Parks Road, Oxford, OX1 3AN, UK
3. Institute for Planetary Materials, Okayama University, 827 Yamada, Misasa, Tottori 682-0193, Japan
4. Department of Environment, Earth and Ecosystems, Open University, Milton Keynes MK7 6AA, UK
5. Centre de Recherches Pétrographiques et Géochimiques, CNRS, UPR 2300, F-54501 Vandoeuvre-lès-Nancy, France
§ Present address: Grant Institute, The King's Buildings, James Hutton Road, Edinburgh EH9 3FE, UK
* Corresponding author (email: ali.bouhifd@uca.fr)

our results and those provided from large volume presses for argon (Fig. S-3a,b).

The chemical compositions of the run products were analysed by an electron microprobe (JEOL JXA-8800R with 4 wavelength dispersive spectrometers) with an accelerating voltage of 15 kV and a beam current of 20 nA (see Table S-1). The chemical analyses for neon with the UVLAMP were carried out at the Open University, UK. A NewWave UP213 combined laser/microscope system uses a 10 Hz quintupled Nd-YAG laser with a wavelength of 213 nm yielding ~10 ns pulses (Heber *et al.*, 2007). The extracted gas was cleaned using three SAES AP-10 getters at 400 °C and room temperature to remove active gases before analysis with a MAP 215–50 noble gas mass spectrometer. Blanks were measured before and after each ablation and all the measured blanks were small with respect to the minimum neon concentrations measured in our samples. For both silicate and metal analyses, the measured ^{22}Ne blanks were $(0.6 \pm 0.1) \times 10^{-12}$ cm^3 STP. To convert measured Ne abundances into concentrations, the volumes of all laser pits were determined by using a non-contact, vertical scanning white light interferometer (Zygo instrument), which has a vertical resolution of ~1 Å and a horizontal resolution of 1 µm.

The experimental conditions, the neon contents of the run products and the resulting partition coefficients for neon are presented in Table 1. Each of the reported results is the average of several spot analyses made from the same phase. During Ne analysis, we ablated the first 2 microns from the surface before starting the quantitative determinations of Ne concentrations. This step is made to avoid the high near-surface concentrations of noble gases (*e.g.*, Bouhifd *et al.*, 2013). Therefore, the neon contents presented here correspond to neon dissolved in the bulk molten phases quenched from HP.

Here we found that the neon solubility in silicate melt dropped by a factor of ~3 (Fig. 1) from ~450 ppm Ne at 6 GPa to ~140 ppm Ne at 10 GPa. This drop of neon solubility can be attributed to the characteristic of silicate melts at high pressures as reported in our study for argon (Bouhifd and Jephcoat, 2006). We also found no evidence for a pressure dependence of Ne solubility in Fe-rich alloys. It is important to note here that the drop of Ne solubility in silicate melt by a factor of 3 will only vary the D_{Ne} coefficient from 3×10^{-2} at 6 GPa (before the drop of Ne solubility in the silicate melt) to 9.8×10^{-2} at 10 GPa (after the drop of Ne solubility). The

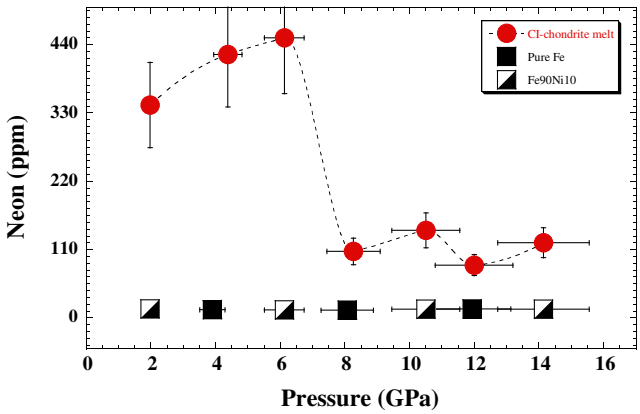

Figure 1 Neon concentrations in CI-chondrite melt, Fe and $Fe_{90}Ni_{10}$ alloy at high pressures. The reported Ne contents represent the average of 5 to 20 analyses. Error bars correspond to 1σ (ranging from 5 to 20 %) of the average of the chemical analyses and to 10 % of the nominal pressures reported. For the metallic phase no pressure dependence is observed and the average value of Ne concentrations is 13.5 ± 0.8 ppm.

variation of D_{Ne} of less than one order of magnitude was taken into account in our calculations and was found not to affect the main conclusion of the present work. Previous studies show that the core can be a plausible source for light noble gases using much lower (~10^{-4}) partition coefficients of He and Ne, meaning that the metal-silicate partition coefficients of noble gases are not the only limiting factor. The main controlling factor being the abundances of noble gases in the proto-Earth (Porcelli and Halliday, 2001; Trieloff and Kunz, 2005).

Measurements of Ne partitioning between metal and silicate have been reported by Matsuda *et al.* (1993) and Sudo *et al.* (1994). These studies indicate high D_{Ne} of ~10^{-1} at P ~0.5 GPa that decreased with increasing pressure to near 10^{-3} at 6 GPa. At about 2 GPa, our D_{Ne} value is similar to that determined by Matsuda *et al.* (1993). However, at pressures ≥2 GPa, we do not observe the systematic decrease in the D_{Ne} coefficients, instead our results indicate higher D_{Ne} coefficients of ~10^{-1} at pressures >8 GPa, which is little dependent on pressure (Fig. 2). This behaviour is similar to that of helium for which we found that D_{He} coefficients are constant over a wide range

Table 1 Neon concentrations (ppm) in molten CI-chondrite and Fe-rich alloys liquids. Values in bold (either for metallic or silicate phases) are linear interpolations between the two nearest experimental pressure data.

P (GPa)	T (K)	Ne contents (ppm)	Ne contents (ppm)	D_{Ne}
		CI-Chondrite melt	Fe-rich alloy liquids	
			$Fe_{90}Ni_{10}$ alloy	
2.0	2400	342 (±25)	14.3 (±1.3)	4.2 (±0.7) × 10^{-2}
4.4	2400	424 (±36)	**13.4 (±1.0)**	3.2 (±0.5) × 10^{-2}
6.1	2500	451 (±32)	12.8 (±1.0)	2.8 (±0.4) × 10^{-2}
8.3	2450	107 (±9)	**12.1 (±1.0)**	1.1 (±0.2) × 10^{-1}
10.5	2500	141 (±15)	13.8 (±1.5)	9.8 (±2.1) × 10^{-2}
12.0	2500	85 (±8)	**14.0 (±1.5)**	1.6 (±0.3) × 10^{-1}
14.1	2700	121 (±14)	14.0 (±2.0)	1.2 (±0.3) × 10^{-1}
			Pure Iron	
3.9	2200	**420 (±40)**	13.4 (±1.0)	3.2 (±0.5) × 10^{-2}
8.1	2200	**110 (±10)**	12.1 (±1.0)	1.1 (±0.2) × 10^{-1}
11.9	2300	**85 (±10)**	14.4 (±1.4)	1.7 (±0.3) × 10^{-1}

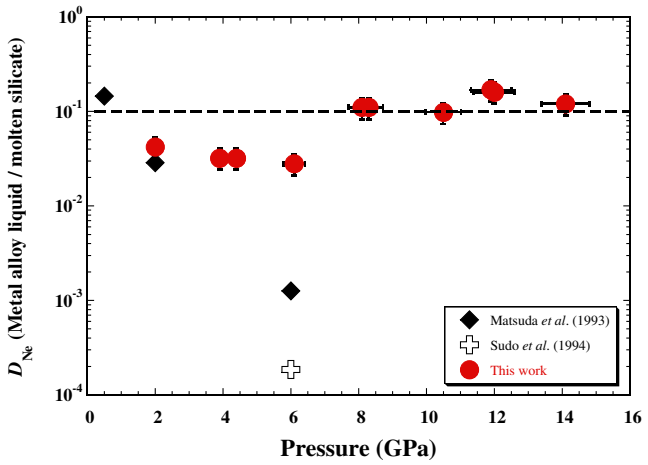

Figure 2 Partition coefficients of Neon, D_{Ne} (wt. % of Ne in metallic phase / wt. % of Ne in silicate) between molten silicate and iron-rich metal liquids as a function of pressure. The average value of our experiments at high pressure is represented by the dashed line. The previous data from Matsuda *et al.* (1993) and Sudo *et al.* (1994) are also plotted. At this stage the discrepancy between data sets at 6 GPa is unknown.

of pressure up to 40 GPa (Bouhifd *et al.*, 2013). We assume thus that the D_{Ne} is within 10^{-2}–10^{-1} at the conditions of Earth's core formation that can reach conditions in the range of 30–70 GPa and 3500 K as determined from moderately siderophile elements.

Assuming a global magma ocean during core formation, our experimental solubilities of Ne and He into a chondritic melt show that under a hot, dense atmosphere from which volatiles are dissolved, such a magma ocean would have been enriched in He with respect to Ne. The reported [He/Ne] ratio (wt. % of He/wt. % of Ne in chondritic melt) shows a negligible dependence on pressure up to 17 GPa with an average of 6 ± 2 (Fig. 3). Because the solubility factor ratio of He by Ne is at most 2 (*e.g.*, Jambon *et al.*, 1986), an early magma ocean would have presented a ratio $^3He/^{22}Ne$ within 2.5–5, reflecting up to two global melting events during the first 100 million years of Earth's history (Tucker and Mukhopadhyay, 2014). For the estimate above, we consider that the initial $^3He/^{22}Ne$ ratio is that of the solar nebula or of implanted solar wind during the early

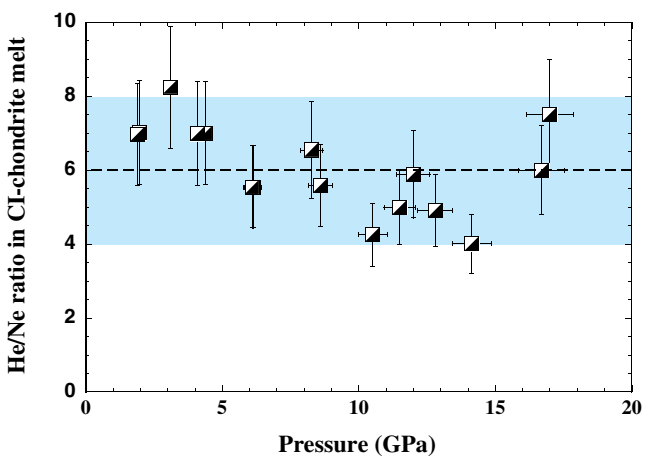

Figure 3 He/Ne ratio (wt. % of He in the melt / wt. % of Ne in the melt) in CI-chondrite melt at high pressures.

solar system, around 1.50 ± 0.06, and 0.9 ± 0.1, respectively (*e.g.*, Yokochi and Marty, 2004; Heber *et al.*, 2009; Raquin and Moreira, 2009; Tucker and Mukhopadhyay, 2014).

In order to evaluate the potential of He and Ne sequestration by the core, it is necessary to estimate the initial abundances of these noble gases on proto-Earth. In the early part of Earth's history, high concentrations of He and Ne that might have existed as Xe isotopes indicate extensive losses of volatile elements from the mantle within the first 100 Myr. Such losses appear to have depleted the noble gases by ≥97 %, implying that their initial concentrations in Earth were two orders of magnitude higher than at present (Porcelli *et al.*, 2001; Yokochi and Marty, 2005). The amounts of primitive helium and neon can thus be estimated from the present day ^3He and ^{22}Ne concentrations in the mantle that range between 2.2 and $>14 \times 10^{-10}$ cc STP/g for ^3He and between 4 and $>58 \times 10^{-11}$ cc STP/g for ^{22}Ne (Yokochi and Marty, 2004; Moreira and Kurz, 2013). We can thus estimate that ^3He primitive mantle's concentrations are in the range of $\sim 10^{12}$ ^3He atoms/g. In addition, the initial Earth $^3He/^4He$ ratio was around $120 \times R_A$ (where $R_A = 1.39 \times 10^{-6}$ is the atmospheric ratio) if solar nebula was trapped in the mantle; or $330 \times R_A$ that represents the solar wind ratio, provided that terrestrial He was derived from solar wind implantation of accreting materials (Porcelli *et al.*, 2001).

By considering the values reported above, abundances of about 2.7×10^{12} ^3He atoms/g and 2.9×10^{12} ^{22}Ne atoms/g in the early Earth's mantle are very plausible. By taking these values as the initial ^3He and ^{22}Ne abundances at time of the core formation, and the measured D_{He} and D_{Ne}, ^3He and ^{22}Ne in the early core could have been between 1.3×10^{10} and 4.6×10^{10} ^3He atoms/g, and between 8.1×10^{10} and 4.9×10^{11} ^{22}Ne atoms/g, respectively. These estimates indicate that the Earth's early core might have had a $^3He/^{22}Ne$ ratio lower than 0.6. During core formation, the $^3He/^{22}Ne$ ratio of the mantle should be within the range 2.5–5, and the metal-silicate partition coefficient of the He/Ne ratio is about 5×10^{-2} (Fig. S-9) leading to a $^3He/^{22}Ne$ ratio within the core in the range of 0.12–0.25. We can thus conclude that the Earth's core must have inherited low $^3He/^{22}Ne$ ratio (<0.6), and any contribution from the core to the OIBs source regions has the potential to lower their $^3He/^{22}Ne$ ratios.

The measured high $^3He/^4He$ and low $^3He/^{22}Ne$ ratios observed now in some OIBs (such as Hawaii) could be the result from mixing of He and Ne from a small core component with radiogenic ^4He and residual ^3He and ^{22}Ne from the mantle. Our new estimates, based on the ratio of the fluxes of noble gases in OIBs to their concentrations in the core, would require that less than 1 % of the mass of the core should have released its primordial light noble gases.

Since significant amounts of siderophile elements are incorporated in the core, additions of core material to the OIBs would impact these elements. For modern OIBs, tungsten isotopic data negatively correlate with $^3He/^4He$ ratios (Mundl *et al.*, 2017). This correlation can indicate core-mantle interaction with transfer of the high $^3He/^4He$ and low ^{182}W signature of the outer core to the source of the OIBs. A similar conclusion was reached in a more recent study by Rizo *et al.* (2019) where they found that core-mantle exchange might be facilitated by exsolution of W-rich, Si-Mg-Fe oxides from the core into the mantle. A correlation between the highest $^3He/^4He$ values and the highest $^{186}Os/^{188}Os$ ratios in Hawaii was also used as an evidence for a core contribution to He and Os (Walker *et al.*, 1995). However, subsequent studies in other OIBs show that this evidence in OIBs cannot be uniquely tied to the core (Luguet *et al.*, 2008). Clearly, the debate over core-mantle exchanges has some way to go, but the present study shows that the early Earth's core

could have incorporated helium and neon making it a potential supplier of light noble gases into deep-rooted mantle plumes. Also the Earth's core must have inherited high $^{3}He/^{4}He$ ratios (in the range 120–330) and low $^{3}He/^{22}Ne$ ratios (<0.6), and the core maintained high and low, $^{3}He/^{4}He$ and $^{3}He/^{22}Ne$ ratios, respectively, throughout Earth's history.

Acknowledgements

To the memory of our friend and colleague Pete Burnard with whom we have had many discussions about the origin of noble gases on Earth. We would like to thank Steve Parman and an anonymous reviewer for comments and suggestions that help us to improve our manuscript. MAB acknowledges the support of a NERC and the PNP-CNRS program. This work was also supported by NERC grants to APJ. This is Laboratory of Excellence ClerVolc contribution number 429.

Editor: Helen Williams

Additional Information

Supplementary Information accompanies this letter at http://www.geochemicalperspectivesletters.org/article2028.

Cite this letter as: Bouhifd, M.A., Jephcoat, A.P., Porcelli, D., Kelley, S.P., Marty, B. (2020) Potential of Earth's core as a reservoir for noble gases: Case for helium and neon. *Geochem. Persp. Let.* 15, 15–18.

References

Armytage, R., Jephcoat, A.P., Bouhifd, M.A., Porcelli, D. (2013) Metal-silicate partitioning of iodine at high pressures and temperatures: implications for the Earth's core and ^{129}Xe budgets. *Earth and Planetary Science Letters* 373, 140–149.

Bouhifd, M.A., Jephcoat, A.P. (2006) Aluminium control of argon solubility in silicate melts under pressure. *Nature* 439, 961–964.

Bouhifd, M.A., Jephcoat, A.P., Heber, V.S., Kelley, S.P. (2013) Helium in Earth's early core. *Nature Geoscience* 6, 982–986.

Heber, V.S., Brooker, R.A., Kelley, S.P., Wood, B.J. (2007) Crystal-melt partitioning of noble gases (helium, neon, argon, krypton and xenon) for olivine and clinopyroxene. *Geochimica et Cosmochimica Acta* 71, 1041–1061.

Heber, V.S., Wieler, R., Baur, H., Olinger, C., Friedmann, T.A., Burnett, D.S. (2009) Noble gas composition of the solar wind as collected by the Genesis mission. *Geochimica et Cosmochimica Acta* 73, 7414–7432.

Jambon, A., Weber, H., Braun, O. (1986) Solubility of He, Ne, Ar, Kr and Xe in a basalt melt in the range 1250–1600 °C: Geochemical implications. *Geochimica et Cosmochimica Acta* 50, 401–408.

Jephcoat, A.P., Bouhifd, M.A., Porcelli, D. (2008) Partitioning experiments in the laser-heated diamond anvil cell: volatile content in the Earth's core. *Philosophical Transactions Royal Society A* 366, 4295–4314.

Luguet, A., Pearson, D.G., Nowell, G.M., Dreher, S.T., Coggon, J.A., Spetsius, Z.V., Parman, S.W. (2008) Enriched Pt-Re-Os isotope systematics in plume lavas explained by metasomatic sulfides. *Science* 319, 453–456.

Marty, B. (2012) The origins and concentrations of water, carbon, nitrogen and noble gases on Earth. *Earth and Planetary Science Letters* 313–314, 56–66.

Matsuda, J., Sudo, M., Ozima, M., Ito, K., Ohtaka, O., Ito, E. (1993) Noble gas partitioning between metal and silicate under high pressures. *Science* 259, 788–790.

Moreira, M. (2013) Noble gas constraints on the origin and evolution of Earth's volatiles. *Geochemical Perspectives* 2, 229–403.

Moreira, M., Kurz, M.D. (2013) Noble gases as tracers of mantle processes and magmatic degassing. In: Burnard, P. (Ed.) *The Noble Gases as Geochemical Tracers*. Advances in Isotope Geochemistry. Springer-Verlag, Berlin, Heidelberg, 371–391.

Mukhopadhyay, S. (2012) Early differentiation and volatile accretion recorded in deep-mantle neon and xenon. *Nature* 486, 101–104.

Mundl, A., Touboul, M., Jackson, M.G., Day, J.M.D., Kurz, M.D., Lekic, V., Helz, R.T., Walker, R.J. (2017) Tungsten-182 heterogeneity in modern ocean island basalts. *Science* 356, 66–69.

Pepin, R.O., Porcelli, D. (2006) Xenon isotope systematics, giant impacts, and mantle degassing on the early Earth. *Earth and Planetary Science Letters* 250, 470–485.

Porcelli, D., Halliday, A.N. (2001) The core as a possible source of mantle helium. *Earth and Planetary Science Letters* 192, 45–56.

Porcelli, D., Wollun, D., Cassen, P. (2001) Deep Earth rare gases: initial inventories, capture from the solar nebula, and losses during Moon formation. *Earth and Planetary Science Letters* 193, 237–251.

Raquin, A., Moreira, M. (2009) Atmospheric $^{38}Ar/^{36}Ar$ in the mantle: implications for the nature of the terrestrial parent bodies. *Earth and Planetary Science Letters* 287, 551–558.

Rizo, H., Andrault, D., Bennett, N.R., Humayun, M., Brandon, A., Vlastelic, I., Moine, B., Poirier, A., Bouhifd, M.A., Murphy, D.T. (2019) ^{182}W evidence for core-mantle interaction in the source of mantle plumes. *Geochemical Perspectives Letters* 11, 6–11.

Roth, A.S.G., Liebske, C., Maden, C., Burton, K.W., Schönbächler, M., Busemann, H. (2019) The primordial He budget of the Earth set by percolative core formation in planetesimals. *Geochemical Perspectives Letters* 9, 26–31.

Sudo, M., Ohtaka, O., Matsuda, J. (1994) Noble gas partitioning between metal and silicate under high pressures: The case of iron and peridotite. In: Matsuda, J. (Ed.) *Noble Gas Geochemistry and Cosmochemistry*. Terra Scientific Publishing Company (TERRAPUB), Tokyo, 355–372.

Trieloff, M., Kunz, J. (2005) Isotope systematics of noble gases in the Earth's mantle: possible sources of primordial isotopes and implications for mantle structure. *Physics of the Earth and Planetary Interiors* 148, 13–38.

Tucker, J.M., Mukhopadhyay, S. (2014) Evidence for multiple magma ocean outgassing and atmospheric loss episodes from mantle noble gases. *Earth and Planetary Science Letters* 393, 254–265.

Walker, R.J., Morgan, J.W., Horan, M.F. (1995) Osmium-187 enrichment in some plumes: evidence for core-mantle interaction? *Science* 269, 819–822.

Williams, C.D., Mukhopadhyay, S., Rudolph, M.L., Romanowicz, B. (2019) Primitive helium is sourced from seismically slow regions in the lower most mantle. *Geochemistry, Geophysics, Geosystems* 20, 4130–4145.

Yokochi, R., Marty, B. (2004) A determination of the neon isotopic composition of the deep mantle. *Earth and Planetary Science Letters* 225, 77–88.

Yokochi, R., Marty, B. (2005) Geochemical constraints on mantle dynamics in the Hadean. *Earth and Planetary Science Letters* 238, 17–30.

Zhang, J., Herzberg, C. (1994) Melting experiments on anhydrous peridotite KLB-1 from 5.0 to 22.5 GPa. *Journal of Geophysical Research* 99, 17729–17742.

Geochemical Perspectives Letters

Potential of Earth's core as a reservoir for noble gases: Case for helium and neon

M.A. Bouhifd, A.P. Jephcoat, D. Porcelli, S.P. Kelley, B. Marty

Supplementary Information

The Supplementary Information includes:

- Starting Materials
- Experimental Techniques
  - Laser Heated Diamond Anvil Cell (LHDAC)
  - Chemical analyses of the run-products
  - Neon in silicate liquids and Fe-rich alloy melts
  - Metal-silicate partition of (He/Ne) ratio
- Table S-1
- Figures S-1 to S-9
- Supplementary Information References

Starting Materials

The CI-model composition (SiO_2 49.6 wt. %, MgO 35.1 wt. %, FeO 8.5 wt. %, Al_2O_3 3.5 wt. %, CaO 3.3 wt. %) is the same starting material used in our previous studies (Bouhifd and Jephcoat, 2006; Bouhifd *et al*., 2013). The proportions of SiO_2, Al_2O_3, MgO and CaO were chosen to be that of model

CI-chondrite. The mix of CI-chondrite with an FeNi-alloy consisted of 66 wt. % of CI-maj, 24 wt. % Fe metal and 10 wt. % Ni metal. Some experiments were performed using only metallic phase consisting on pure Fe (High purity 99.99+%) or FeNiCo (54 wt. % Fe, 29 wt. % Ni, 17 wt. % Co) metal foils that were obtained from "Goodfellow Cambridge Ltd".

Experimental Techniques

Laser Heated Diamond Anvil Cell (LHDAC)

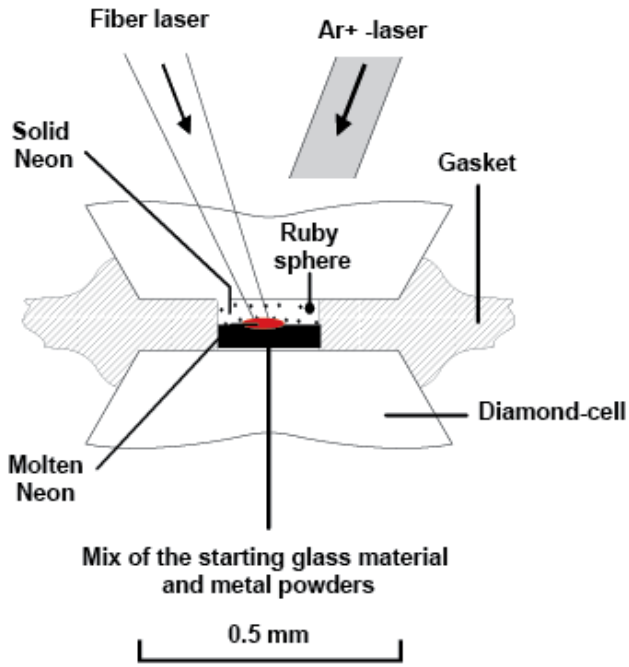

Figure S-1. A typical sample configuration in the Laser Heated Diamond Anvil Cell (LHDAC) for noble gases partitioning experiments (see text for details). Prior to experiments, neon was loaded into the pressure chamber with a high-pressure gas-loading technique at 200 MPa.

For the present experiments we used a set-up similar to that described in previous studies (*e.g.* Jephcoat *et al*., 2008). We used diamond anvils with 500 µm culets, and stainless-steel gaskets pre-indented to a thickness of ~50 µm and drilled to a diameter of ~100 µm. Samples were mounted in the pressure chamber and neon was loaded with a high-pressure gas-loading technique at 200 MPa. Neon served as pressure-transmitting medium for all runs. The samples were heated by a 100 W air-cooled fibre laser with emission centred at 1070 nm (Model R4, SPI Lasers UK Ltd.) for an average of about 10 to 15 minutes of each zone of the sample (Fig. S-1). To reduce the temperature gradient across the samples, a relatively broad, defocused beam (hot-spot size around 20 microns) was used. With this

temperature gradient, the maximum difference between the temperature at the centre and the edge of the laser spot is 200 degrees (which was taken as a conservative uncertainty on the temperature). Temperatures were determined spectro-radiometrically with a fit to a grey-body Planck function. Great care was taken to scan the hot spot slowly over the whole sample, allowing each part of the sample to be heated to the maximum temperature forming uniform melt pools (either silicate or metal). When the laser beam was initially focused on the starting material, the power was increased slowly until the sample was clearly melted. Several criteria can attest of the melting of the samples at high pressure (*e.g.* Chamorro-Perez *et al.*, 1996), and among these criteria the temperatures of our runs were higher by at least 200 degrees in comparison to the liquidus temperature of peridotite with similar chemical composition to our starting material (*e.g.*, Zhang and Herzberg, 1994; and Fig. S-2).

Finally, during the heating stage the surrounding solid neon, that acts as a pressure-transmitting medium, melted by conductive heating from the heated sample, allowing dissolution of Ne into the sample studied, consistent with the melting curve of neon at high pressure (Santamaria-Pérez *et al.*, 2010). Pressures were measured using the ruby fluorescence method and the hydrostatic pressure scale. For each run, the fluorescence emission of one ruby grain at the edge of the gasket hole was systematically recorded at room temperature before and after heating. We did not observe any difference, within an uncertainty of 10 %, between both pressures. However, in our configuration, an increase of a few GPa on top of the nominal pressures can be expected as deduced from similar LHDAC studies (*e.g.* Andrault *et al.*, 1998). The thermal pressure can be estimated by the following equation: $P_{Th} = \alpha K \Delta T$, where α and K are the thermal expansion and bulk modulus, respectively, and ΔT is the difference between run and room temperatures, respectively. By assuming $\alpha \sim 10^{-5}$, and using the 3rd order Birch-Murnaghan equation of state (with K_0 = 26 GPa and K'_0 = 7 as reported by Guillot and Sator (2007) for a similar silicate melt composition), the pressure correction in our experiments at 5 GPa is about 0.6 and 0.8 GPa at 2500 and 3000 K, respectively. The pressure correction at 14 GPa is about 1.5 GPa between 2500 and 3000 K.

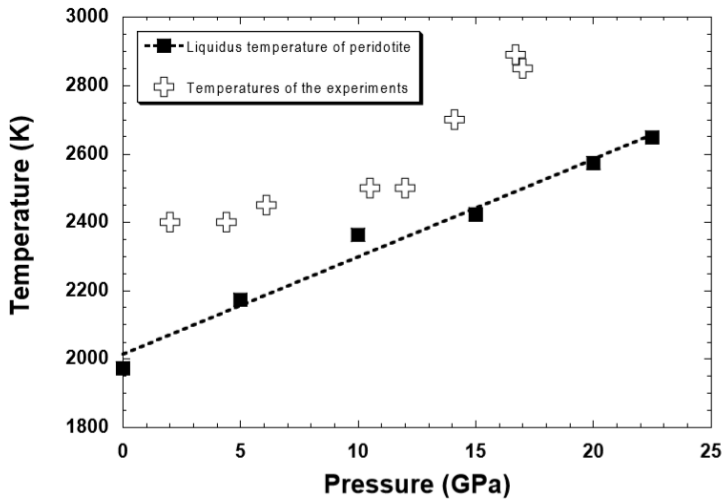

Figure S-2 Temperatures of the experiments in the present study in comparison to the melting temperature of peridotite up to 23 GPa (Zhang and Herzberg, 1994).

Because our experiments are not routine ones the success of our LHDAC technique was demonstrated in our previous studies where we found an excellent agreement between our results and those provided from large volume presses for other volatile elements such as argon (Figs. S-3a – S-3b).

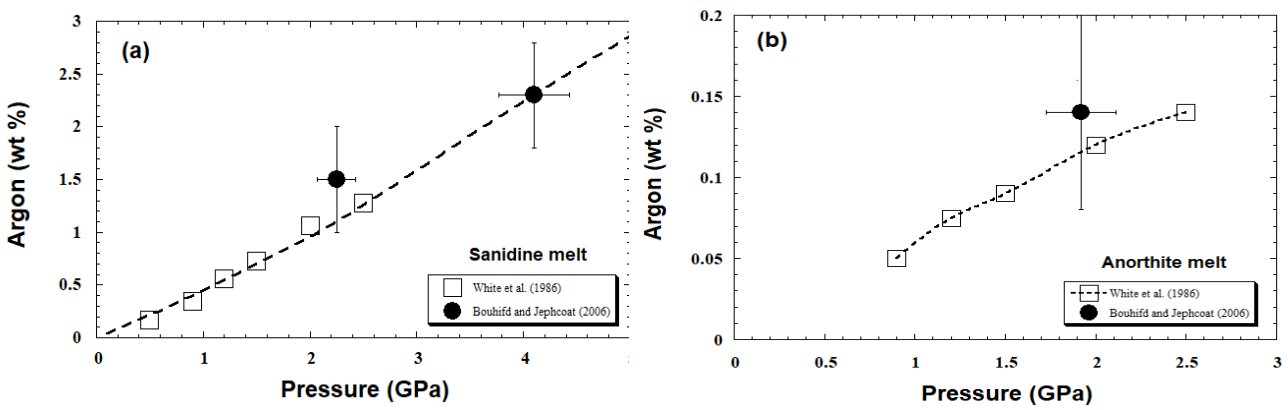

Figure S-3 Ar contents as a function of pressure **(a)** for sanidine melt and **(b)** for anorthite melt. The data from Bouhifd and Jephcoat (2006) are obtained using LHDAC and those of White *et al*. (1986) by using a piston-cylinder apparatus.

Chemical analyses of the Run-Products

Prior to noble gases analyses, the chemical compositions of the run products were analysed by an electron microprobe (JEOL JXA-8800R with 4 wavelength-dispersive spectrometers) with an accelerating voltage of 15 kV and a beam current of 20 nA. Counting times for analyses were about 100s for each analysis. Fe, FeS, Ni and Co metals, orthoclase, jadeite, wollastonite, periclase and corundum were employed as standards.

Table S-1. Chemical composition of the run-products (wt. %). For all our run products we found that the silicate composition is not varying at the present experimental conditions.

Oxides	
SiO_2	47.9 ± 1.2
Al_2O_3	6.2 ± 0.4
FeO	7.1 ± 1.0
MgO	35.5 ± 1.0
CaO	2.8 ± 0.3
Total	**99.5**

Neon analyses in silicate liquids

To determine the partition coefficients of Ne between molten silicate and metal liquid, we consider only the interior bulk concentrations and that we assume to be the equilibrium concentration. So, prior to determine Ne profiles for both phases, we removed the 2 first microns to avoid any high Ne concentrations within the first micrometre depth for both silicate and metal phases. Such high noble gases concentrations near the surface were also observed during our He metal-silicate partitioning study. Note that including the high concentrations near the surface in both silicate and metal leads to similar partition coefficients to those that exclude the surface layer (Bouhifd *et al*., 2013).

All Ne concentrations results presented here represent at least 1 depth profile (with at least 5 individual and up to 20 Ne analyses). The uncertainties on the reported averaged values (1σ) (see Table 1 in the main text) range from 5 to 20 %.

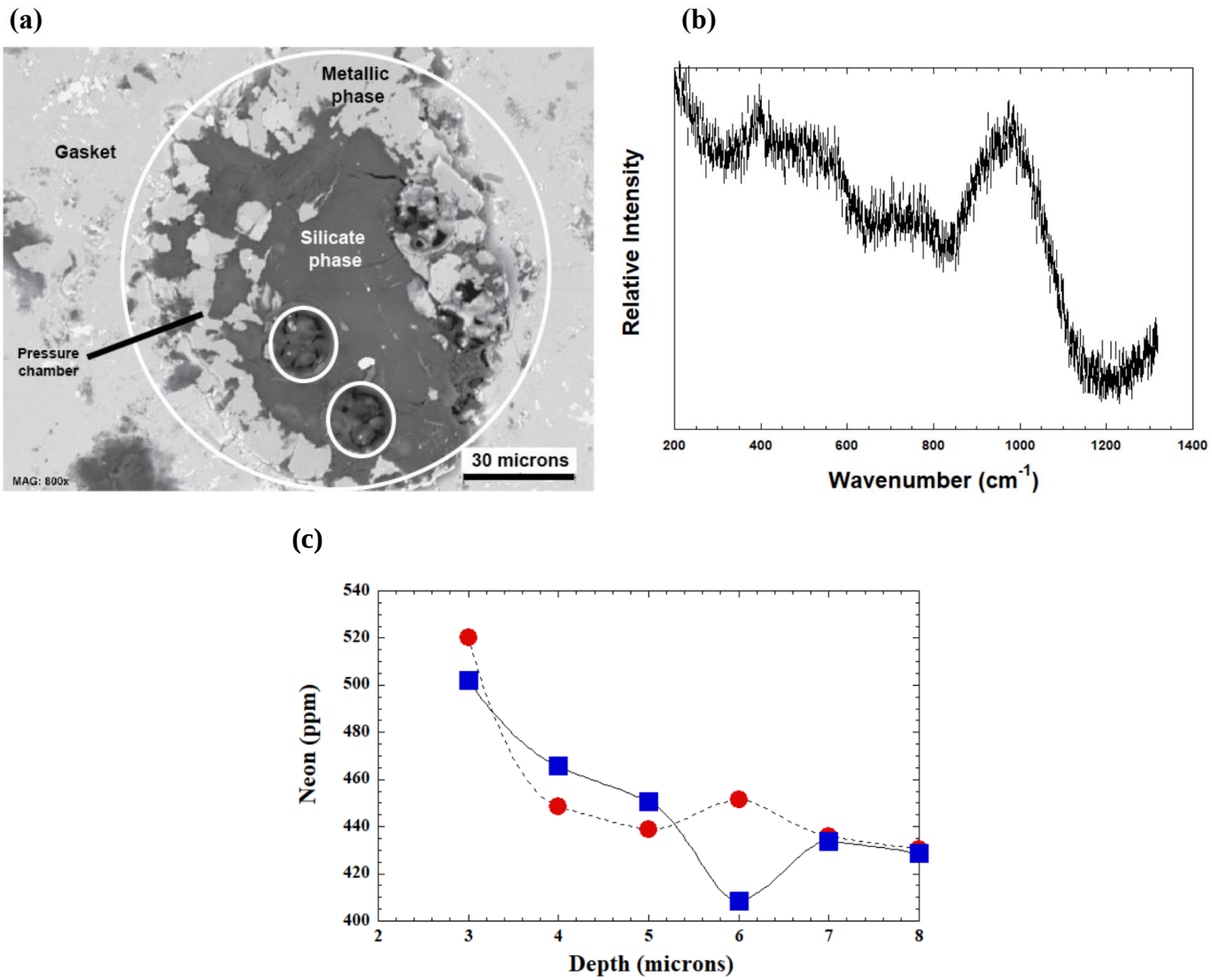

Figure S-4 (a) Back-scattered electron image of run-product quenched from 6.1 GPa and 2500 K. Neon analyses were performed in zones showing a glassy phase formed from quenching the silicate melt from HP. The small white circles show the pits of the laser ablation. **(b)** Raman spectra recorded in zones (glass quenched from HP-HT) prior to neon analyses. **(c)** Depth profiles of Ne concentrations in the silicate phase. Uncertainties are smaller than the symbol sizes (better than 1%) and all data were corrected from the blanks. Lines between symbols serve as a guide only. The two different symbols correspond to different depth profiles within the same run-product reported in Figure S-4a. The average Ne concentration in this sample (6.1 GPa, 2500 K), determined from12 single analyses of 2 profiles, is 451 ± 32 ppm.

For the highest pressures (10 to 16 GPa) of the present work, the Raman study prior to Ne analyses show several features. In the Figure S-5a-b we report a run-product (pure silicate phase) quenched from 10.5 GPa and 2500 K.

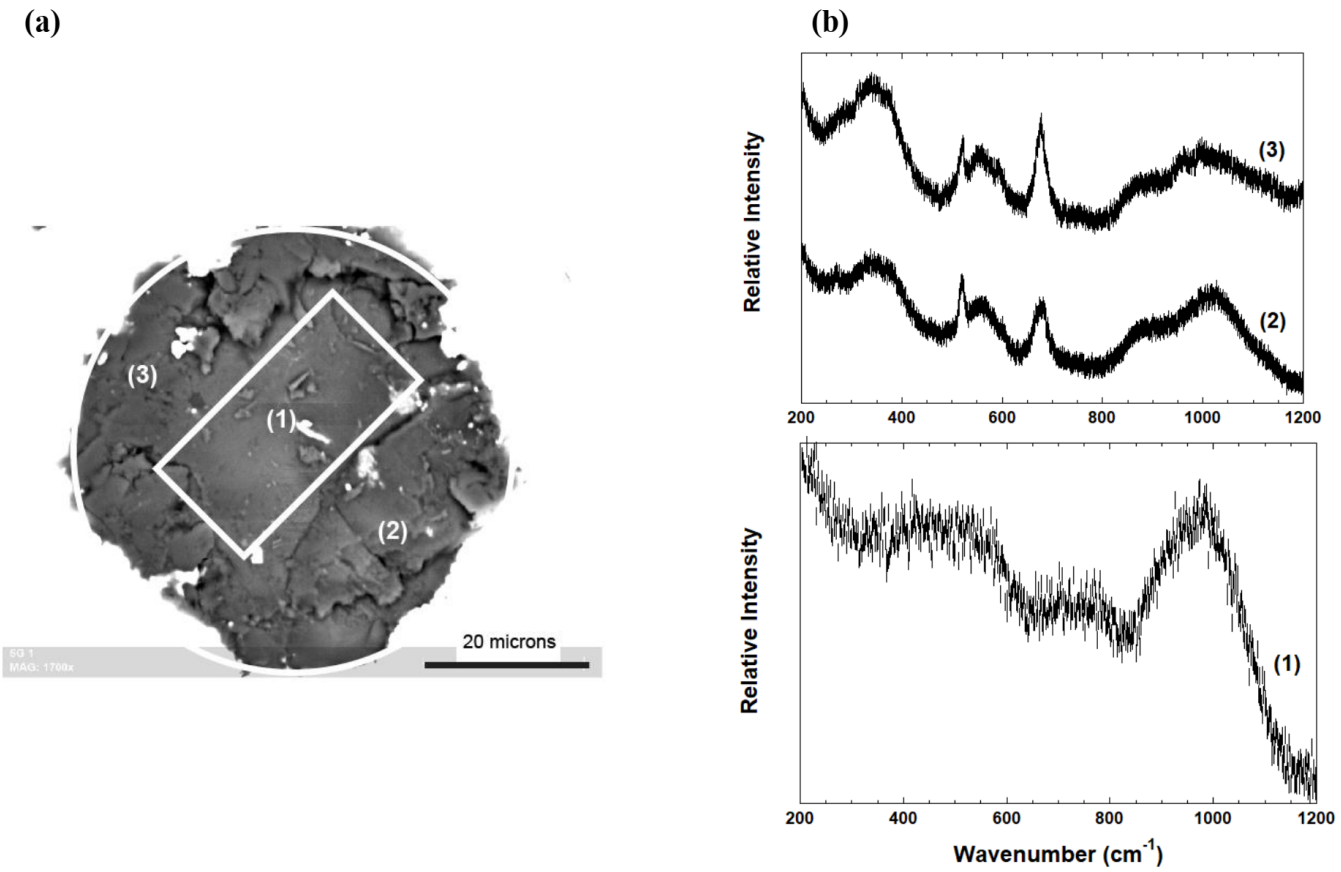

Figure S-5. **(a)** Run-product quenched from 10.5 GPa and 2500 K. Three distinct zones were found in this sample as shown by their respective Raman spectra **(b)**. Zone (1) is a glassy phase, zone (2) is a mix between glass and crystalline phase and zone (3) is a mix between glass and crystalline phases with higher proportion of crystals.

We performed 4 neon profiles on this run-product (2 in zone (1), 1 in zone (2) and 1 in zone (3)) (Fig. S-6). The averaged neon concentrations in zone (1) is 141±15 ppm, in zone (2) is 132±15 ppm and in zone (3) is 120±12 ppm. In zones (2) and (3) that show some recrystallization, the neon concentrations are lower by about 6% and 15% than the concentration for the glassy zone (1). This behaviour is consistent with the study of Niwa *et al*. (2013) on the Ar solubility in SiO_2 melt under high pressures, where they observed a decrease of about 10% of Ar concentration in sample showing crystallization in comparison to a glass quenched from HP-HT. This behaviour is also consistent with the negligible loss of noble gases from the LHDAC samples during the quench. In fact, the much higher thermal diffusivity in a LHDAC (about 10^{-6} to 10^{-7} m^2/s) in comparison to the noble gases diffusion in silicate melts at HP (about 10^{-10} m^2/s) rules out a potential exsolution of noble gases from the heated samples during quenching.

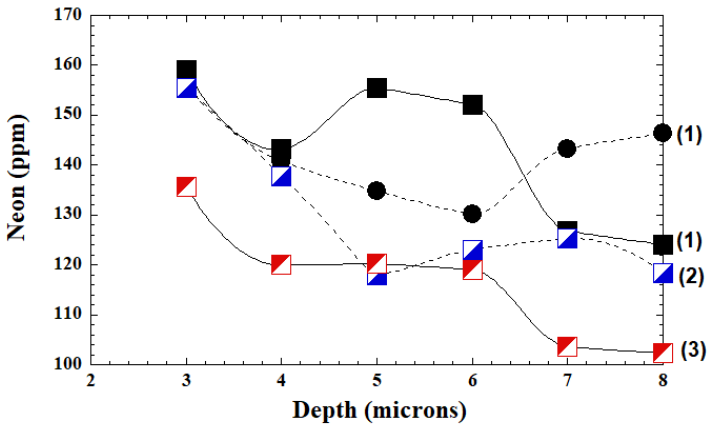

Figure S-6 Depth profiles of Ne concentrations in the silicate phase corresponding to the zones (1), (2) and (3) of the run-product reported in Figure S-5. The partially crystallized zones (2) and (3) contains less Ne by about 6 and 15% in comparison to the glassy zone (1).

Neon in Fe-rich alloy melts

Figure S-7 reports a run-product used to determine Ne concentrations for a molten Fe metal quenched from 8.1 GPa and 2200 K. The two neon profiles show an average neon concentration of 12.1±1.0 ppm.

(a) **(b)**

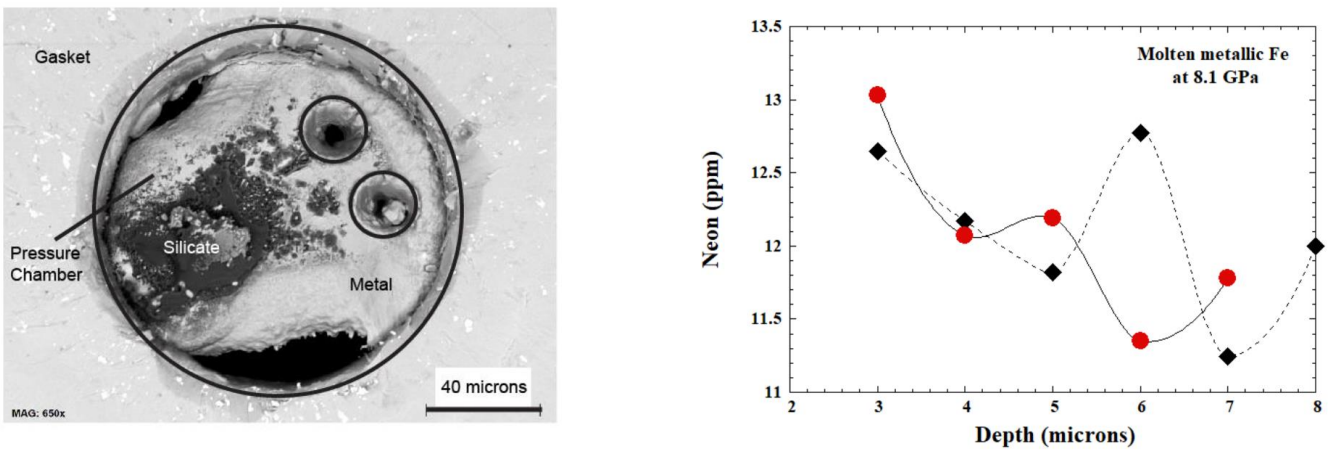

Figure S-7 (a) Back-scattered electron image of run-product analysed for Ne concentrations in metallic Fe. The sample was quenched from 8.1 GPa and 2200 K. **(b)** Depth profiles of Ne concentrations in the metallic phase. The close agreement of the profiles indicates the analytical method is reproducible. Uncertainties are smaller than the symbol sizes (better than 1%) and all data were corrected from the blanks. Lines between symbols serve as a guide only. The different symbols correspond to different depth profiles within the same sample.

Our experiments and analyses show that there is no pressure dependence of neon solubility in Fe-rich alloys, rather it remains relatively constant (within the analytical uncertainties) up to 14 GPa (Figure S-8). All Ne concentrations in metallic phases of this study represent at least 2 depth profiles (with at least 10 individual and up to 20 Ne analyses). The uncertainties on the reported averaged values (1σ) range from 7.5 to 14% (see Table 1 in the main text).

The striking feature here is that we obtain higher concentrations of Ne (13.5±0.8 ppm) in molten Fe-rich alloys in comparison to He concentrations reported in Bouhifd *et al*. (2013). The reason for this behaviour is not understood at this stage but we are planning future experiments where different noble gases will be present simultaneously during metal-silicate partitioning to determine the physical and chemical factors controlling the solubility of noble gases in molten Fe-rich alloys at high pressure.

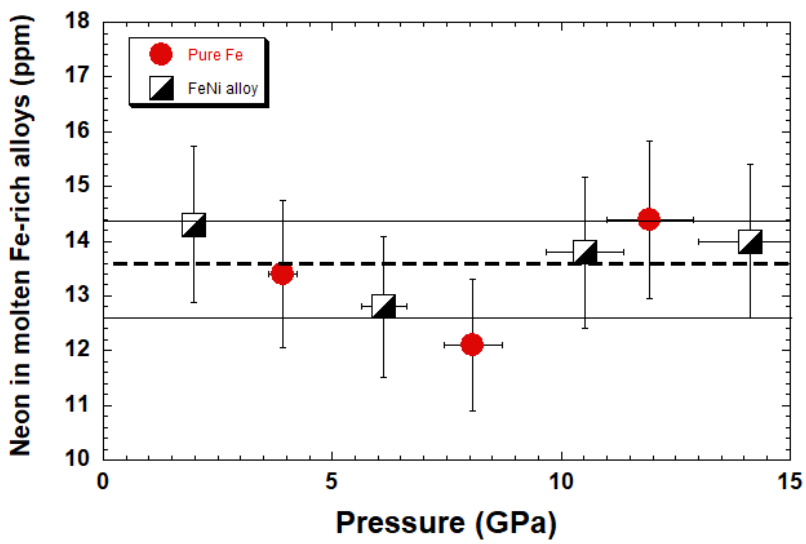

Figure S-8. Neon concentrations in molten metal alloys at high pressures. The reported concentrations are those used to determine the partition coefficients of neon between molten silicate and Fe-rich alloys liquids. We plot constant dashed lines averages of all values of Ne concentrations in metals with the parallel limits representing one standard deviation. The average value for Ne concentrations in molten metal alloys at high pressures is 13.5±0.8 ppm.

Neon and Helium partition coefficients ratio

Combining the metal – silicate partitioning results of Ne and He we observe that $D_{He/Ne}^{metal-Silicate}$ (the ratio of D_{He} over D_{Ne}) is roughly constant and equals to $(5\pm2)\times10^{-2}$. In fact, given the experimental uncertainties, this ratio varies between 2×10^{-2} and 9×10^{-2} (Fig. S-9). In the discussion of our results, we

therefore take D_{He} and D_{Ne} to be within 10^{-3} – 10^{-2} and 10^{-2} – 10^{-1}, respectively, and that $D_{He/Ne}^{metal-Silicate}$ is about 5×10^{-2} during the conditions of Earth accretion and the segregation of its core.

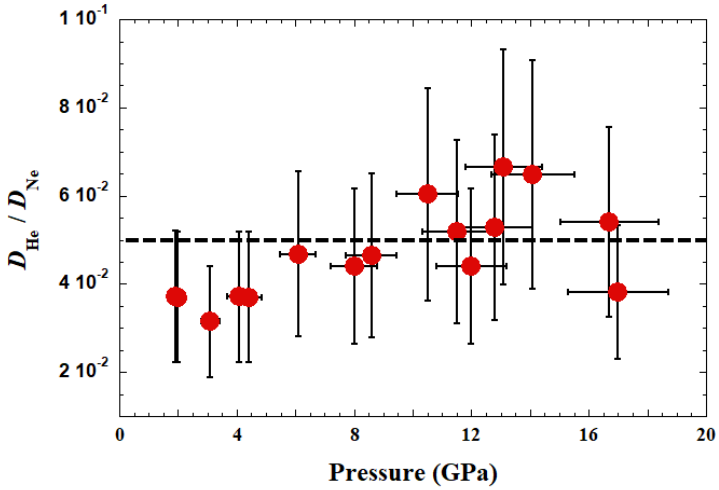

Figure S-9 Metal-silicate partition of (He/Ne) ratio $D_{He/Ne}^{metal-Silicate}$(the ratio of D_{He} over D_{Ne}) versus pressure.

Supplementary Information References

Andrault, D., Fiquet, G., Itié, J.P., Richet, P., Gillet, P., Hausermann, D., Hanfland, M. (1998) Thermal pressure in the laser-heated diamond-anvil cell: an X-ray diffraction study. *European Journal of Mineralogy* 10, 931–940.

Bouhifd, M.A., Jephcoat, A.P. (2006) Aluminium control of argon solubility in silicate melts under pressure. *Nature* 439, 961-964.

Bouhifd, M.A., Jephcoat, A.P., Heber, V.S., Kelley, S.P. (2013) Helium in Earth's early core. *Nature Geoscience* 6, 982-986.

Chamorro-Perez, E., Gillet, P., Jambon, A. (1996) Argon solubility in silicate melts at very high pressures. Experimental set-up and preliminary results for silica and anorthite melts. *Earth and Planetary Science letters* 145, 97-107.

Guillot, B., Sator, N. (2007) A computer simulation of natural silicate melts. Part II: high pressure properties. *Geochimica et Cosmochimica Acta* 71, 4538–4556.

Jephcoat, A.P., Bouhifd, M.A., Porcelli, D. (2008) Partitioning experiments in the laser-heated diamond anvil cell: volatile content in the Earth's core. *Philosophical Transactions Royal Society A* 366, 4295-4314.

Niwa, K., Miyakawa, C., Yagi, T., Matsuda, J. (2013) Argon solubility in SiO_2 melt under high pressures: A new experimental result using laser-heated diamond anvil cell. *Earth and Planetary Science letters* 363, 1-8.

Santamaria-Pérez, D., Mukherjee, D.G., Schwager, B., Boehler, R. (2010) High-pressure melting curve of helium and neon: Deviations from corresponding states theory. *Physical Review B* 81, 214101.

White, B.S., Brearly, M., Montana, A. (1989) Solubility of argon in silicate liquids at high pressures. *American Mineralogist* 74, 513–529.

Zhang, J., Herzberg, C. (1994) Melting experiments on anhydrous peridotite KLB-1 from 5.0 to 22.5 GPa. *Journal of Geophysical Research* 99, 17729-17742.